

# Effect of alumina filler on spherulite growth and ionic conductivity of PEO<sub>9</sub>(LiClO<sub>4</sub>) solid polymer electrolyte

B. A. Karunaratne<sup>1,2,\*</sup>, F. A. E. Nugera<sup>1</sup>, M. A. K. L. Dissanayake<sup>3</sup>,  
G. K. R. Senadeera<sup>3,4</sup> and B.-E. Mellander<sup>5</sup>

<sup>1</sup>Faculty of Applied Science and <sup>2</sup>Faculty of Technology, Rajarata University of Sri Lanka, Mihintale, Sri Lanka

<sup>3</sup>National Institute of Fundamental Studies, Hantana Road, Kandy, Sri Lanka

<sup>4</sup>Department of Physics, The Open University of Sri Lanka, Nawala, Nugegoda, Sri Lanka

<sup>5</sup>Department of Physics, Chalmers University of Technology, Gothenburg, Sweden

**The effect of incorporation of alumina on conductivity and *in situ* growth of spherulites in (PEO)<sub>9</sub>LiClO<sub>4</sub> solid polymer electrolyte was studied using polarized microscopy, impedance and infrared spectroscopy. Fourfold enhancement in ionic conductivity correlated with increase in the amorphous nature of the polymer electrolyte was observed with the addition of 15 wt% of alumina having 5.5 nm pore size. The addition of 5 wt% of alumina with pore size <10 μm, increased the ionic conductivity by nearly 3%. Filler particles may act as nuclei for the spherulites, while preventing the recrystallization tendency of the polymer and hence increase its conductivity.**

**Keywords:** Alumina filler, ionic conductivity polymer electrolyte, polyethylene oxide, spherulite.

SOLID polymeric electrolytes based on polyethylene oxide (PEO) with lithium salts attract widespread attention due to their potential uses in many practical applications such as rechargeable batteries, electrochromic displays, etc.<sup>1-5</sup>. However, the low amorphous nature and poor Li<sup>+</sup> ion conductivity, especially at ambient temperatures, hinders their practical applications. One of the crucial factors which determines the conduction mechanism of these PEO-based polymer electrolytes is the amorphous nature of the polymer chain. The coordination of oxygen atoms in the ether oxygen bond and the lithium ions provides a pathway for the Li<sup>+</sup> ion transportation by thermal motion of the polymer segments in the long chain of the polymer matrix. However, PEO-based solid polymer electrolytes suffer from low ionic conductivity ( $\sigma$ ), especially at room temperature. In order to enhance the ionic conductivity by reducing the crystalline nature of these solid polymer electrolytes, various strategies, such as the use of plasticizers<sup>6</sup>, filler<sup>7-9</sup>, ionic liquids<sup>10,11</sup>, low-molecular weight oligomers<sup>12</sup>, etc. have been employed. Among these, it has been shown that migration of charge

carriers could effectively enhance by adding filler materials to the polymer electrolyte while reducing the degree of the crystallinity. The fundamental unit in a crystalline polymer is called a 'spherulite' which is made up of helices of PEO<sup>13</sup>. A spherulite is a circular-shaped unit with spherically symmetric arrays of lamellar crystals within the amorphous phase. These spherulites grow radially from a centre called the 'nucleus'. The nucleus may be formed by density variation caused by the initial chain arrangement process or by an impurity present in the system. If the nucleation density is high, then the symmetry of the spherulite is lost. This is because they impinge on their neighbours. One polymer chain may contribute to the formation of more than one spherulite<sup>14</sup>. The size of the spherulite may vary from micrometres to a few millimetres. The formation of spherulite can be divided into two stages: nucleation stage and growth stage. Nucleation stage may be heterogeneous or homogeneous. For instance, in the filler-free (PEO)<sub>9</sub>LiClO<sub>4</sub> system, homogeneous nucleation exits. Initially, the PEO chains form the nucleus by the local relaxation process and segmental motion. Then the growth of the nucleus occurs to form the spherulite. When filler particles like alumina are introduced to the system, heterogeneous and homogeneous nucleation may occur. Thus introducing particles can act as the nucleus for spherulite formation. Addition of ceramic particles such as Al<sub>2</sub>O<sub>3</sub>, TiO<sub>2</sub> and SiO<sub>2</sub> has shown high ionic conductivity values in PEO-based systems<sup>15-19</sup>. The purpose of adding ceramic fillers is to decrease the crystallinity, and thus increase the amorphous nature of the polymer in order to enhance conductivity. The addition of filler particles has a major influence on both stages of spherulite formation and growth. Some particles may act as nucleons for the formation of spherulites, while the rest may prevent recrystallization tendency of PEO polymer chains. This occurs through Lewis acid-base interactions with cations and anions present in the system, which results in decrease in the growth rate of the spherulites. Even though large number of research publications are available on conductivity

\*For correspondence. (e-mail: anandaxrf@yahoo.com)

enhancement with different filler materials, there are only few studies on the growth of spherulites and conductivity enhancement of PEO-based systems. Therefore, in this study, PEO-based solid polymer electrolytes have been synthesized by incorporating  $\text{Al}_2\text{O}_3$  with different particle sizes and characterized mainly using electrical impedance spectroscopy measurements and polarization microscopy. These methods were employed to study the effect of addition of ceramic fillers on the conductivity of the system and on spherulite growth.

## Materials and methods

Poly(ethylene oxide) (PEO) with an average molecular weight ( $M_w$ ) of  $4 \times 10^6 \text{ g mol}^{-1}$ , lithium perchlorate ( $\text{LiClO}_4$ ) and alumina ( $\text{Al}_2\text{O}_3$ ) with different pore sizes (5.5 nm and  $<10 \mu\text{m}$ , purchased from Sigma Aldrich) were vacuum-dried under  $50^\circ\text{C}$ ,  $60^\circ\text{C}$  and  $200^\circ\text{C}$  for 24 h respectively.

### Preparation of polymer electrolytes

Different polymer electrolyte compositions were synthesized by dissolving predetermined amounts of PEO and  $\text{LiClO}_4$  in acetonitrile using solvent cast method. Stereo-metric representation of the polymer–salt complex is:  $(\text{PEO})_n M_a X_b$ , where the inorganic salt is represented by  $M_a X_b$  and the ratio between the cations ( $M^{b+}$ ) and ether atoms in the polymeric chain is represented by  $n$ . In order to obtain the  $(\text{PEO})_9 \text{LiClO}_4$  electrolyte composition, the amount of salt ( $w$ ) added to 0.5 g of PEO is calculated using the following equation

$$w = \frac{M_w \text{ of salt}}{n(M_w \text{ of PEO unit})} \times 0.5 \text{ g,}$$

where  $M_w$  is the molecular weight.

The composite solid electrolytes denoted by  $(\text{PEO})_9 \text{LiClO}_4 + \text{wt}\% \text{ Al}_2\text{O}_3$  were prepared by adding wt% of  $\text{Al}_2\text{O}_3$  of the total  $(\text{PEO})_9 \text{LiClO}_4$  weight. In order to dissolve the salt and polymer, 1 ml of acetonitrile was used as the solvent. The solvent was totally evaporated by keeping the samples at  $60^\circ\text{C}$  under vacuum conditions.

### Measurement of ionic conductivity using AC impedance technique

Total ionic conductivity of different polymer electrolyte compositions was measured (Schlumberger 2460 impedance gain phase analyzer) in the frequency range between 20 Hz and 10 MHz by sandwiching disk-shaped polymer electrolyte samples between two stainless-steel blocking electrodes. The temperature of each sample was increased from  $0^\circ\text{C}$  to  $100^\circ\text{C}$ . Measurements were taken at  $10^\circ\text{C}$  intervals after the sample reached thermal equilibrium.

### Polarized optical microscopy

The morphological structure of the electrolytes was observed employing polarized light microscopy (Euro-nex, Model No:D.C. 1300). A thin film of the electrolyte deposited on a microscope slide glass was used for these observations. The formation of spherulites during transition from melting stage ( $60^\circ\text{C}$ ) to room temperature ( $27^\circ\text{C}$ ) was observed for pure PEO,  $(\text{PEO})_9 + \text{LiClO}_4$ , and for the systems containing  $\text{Al}_2\text{O}_3$ . Heating was done using a homemade mini heater.

### Fourier transform infrared spectroscopy analysis

Fourier transform infrared (FT-IR) spectra of the electrolyte samples were obtained (NICOLET 6700 spectrometer) to identify different interactions among the components in the electrolyte.

## Results and discussion

### Temperature dependence of ionic conductivity of the polymeric systems

Figure 1 shows the temperature dependence of ionic conductivity of the  $(\text{PEO})_9 \text{LiClO}_4 + x \text{ wt}\%$  polymeric systems with alumina having 5.8 nm and  $<10 \mu\text{m}$  pore size. While the amount of alumina with pore size 5.8 nm was varied as  $x = 0, 5, 10, 12.5, 15$  and  $17.5$ , the amount of alumina with pore size  $<10 \mu\text{m}$  was varied as  $x = 0, 2.5, 5, 7.5, 10$  and  $15$ .

As depicted in Figure 1, in both systems the addition of filler increases the conductivity of the polymer electrolyte and follows the Arrhenius-type of behaviour as observed by several researchers<sup>20,21</sup>. Further increase of alumina content reduced the conductivity in both the systems studied. The highest conductivity of  $7.62 \times 10^{-6} \text{ S cm}^{-1}$  at room temperature was achieved with the electrolyte system containing 15% alumina ( $\phi = 5.8 \text{ nm}$ ), whereas the system with no alumina,  $(\text{PEO})_9 \text{LiClO}_4$ , showed room temperature conductivity of  $2.03 \times 10^{-6} \text{ S cm}^{-1}$ . The addition of alumina with pore size  $<10 \mu\text{m}$  increases the conductivity of the pristine polymer electrolyte up to  $6.58 \times 10^{-6} \text{ S cm}^{-1}$ . Therefore, nearly 4% enhancement in the conductivity was achieved with these solid-state polymeric systems. It can also be observed from Figure 1, that the phase transition from semi-crystalline to amorphous phase occurs around  $60^\circ\text{C}$  for  $(\text{PEO})_9 \text{LiClO}_4$ . It disappears in the samples containing alumina and appears to obey the Vogel–Tamman–Fulcher (VTF) behaviour, indicating its amorphous nature<sup>19,20</sup>.

Figure 2 shows the conductivity isotherms of the above two polymeric systems in the temperature range from  $27^\circ\text{C}$  to  $100^\circ\text{C}$ . Figure 2a shows the conductivity isotherms of  $(\text{PEO})_9 \text{LiClO}_4$  with 5.8 nm size alumina

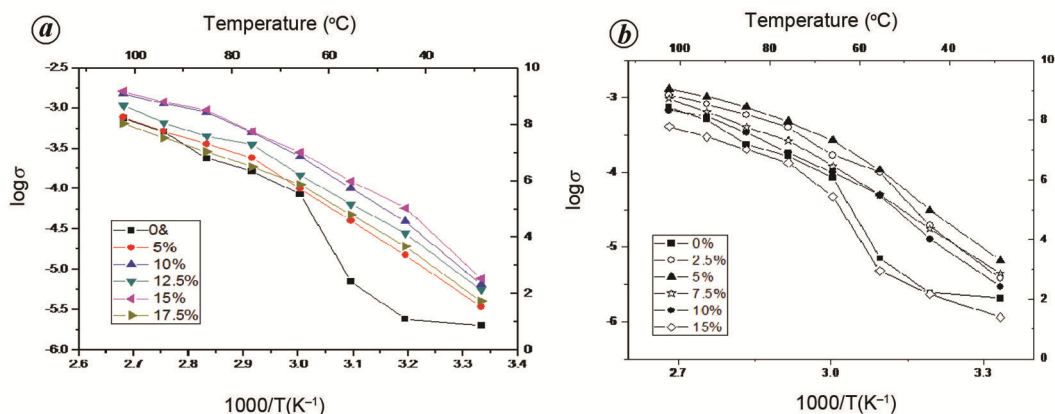


**Figure 1.** Temperature dependence of the conductivity of (PEO)<sub>9</sub>LiClO<sub>4</sub> polymer electrolyte with different wt% of (a) 5.8 nm and (b) <10 μm sizes alumina.

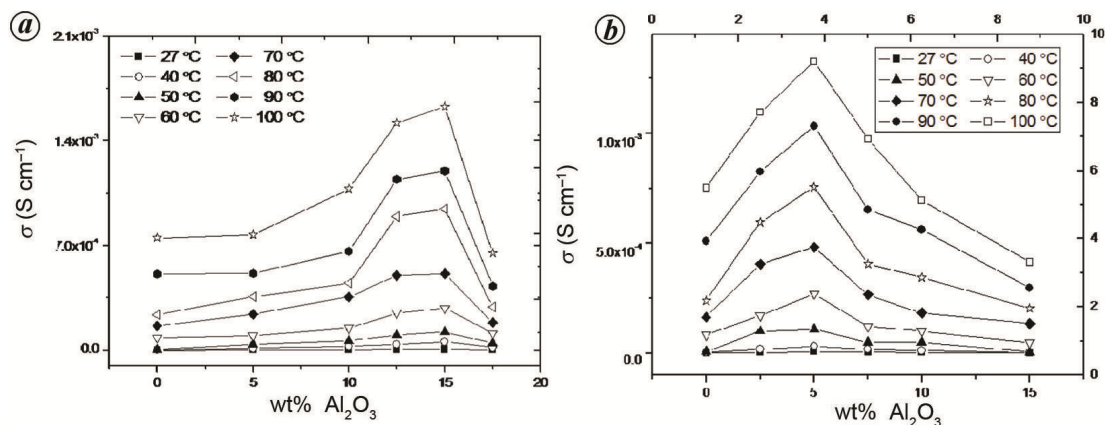


**Figure 2.** Conductivity isotherms of (PEO)<sub>9</sub>LiClO<sub>4</sub> polymeric system with (a) 5.8 nm and (b) <10 μm sizes Al<sub>2</sub>O<sub>3</sub>.

particles, whereas Figure 2b shows the conductivity of the electrolyte with larger alumina particles of pore size <10 μm. As can be seen from Figure 2a, 15 wt% Al<sub>2</sub>O<sub>3</sub> with pore size 5.8 nm gives the highest conductivity, whereas the system with larger alumina particles of pore size <10 μm gives the highest conductivity in 5 wt% composition.

### POM results

The spherulite morphology of pure PEO was observed employing polarized optical microscopy (POM). Figure 3 displays the POM images showing the growth of PEO spherulites in pure PEO which is heated up to 62°C and allowed to cool in air with a cooling rate of 4°C/min during recrystallization. As can be seen from the Figure 3, during the cooling process many spherulites grow simultaneously and impinge with their neighbours forming regions of continuous crystalline phase and lose their symmetry. Spherulites found at room temperature generally have

diameters in the range 80–100 μm. As shown in Figure 3a and k, when the sample is heated and allowed to cool to room temperature, the diameter of the spherulites becomes larger than that of the unheated polymer matrix.

Figure 4 shows the sequence of images in the cooling process for the polymer electrolyte (PEO)<sub>9</sub>LiClO<sub>4</sub> heated up to 55°C and allowed to cool in air with a cooling rate of 3°C/min. Only few spherulites can be seen during the cooling process. One of the reasons for this might be the difficulty in forming nuclei by the spontaneous arrangement. These spherulites grow quickly as soon as the nuclei are formed. The last image in Figure 4 which was taken 570 sec after heating, shows a spherulite with diameter exceeding 200 μm.

Figure 5 shows POM images of the growth of spherulites with addition of Al<sub>2</sub>O<sub>3</sub> (5.8 nm pore size, 150 mesh) and Al<sub>2</sub>O<sub>3</sub> (<10 μm). From these images it is clear that the size of the spherulites decreases and the number of spherulites increases with increase in concentration of the filler. The average diameter of the spherulites decreases to about 8–20 μm. The average diameter of the

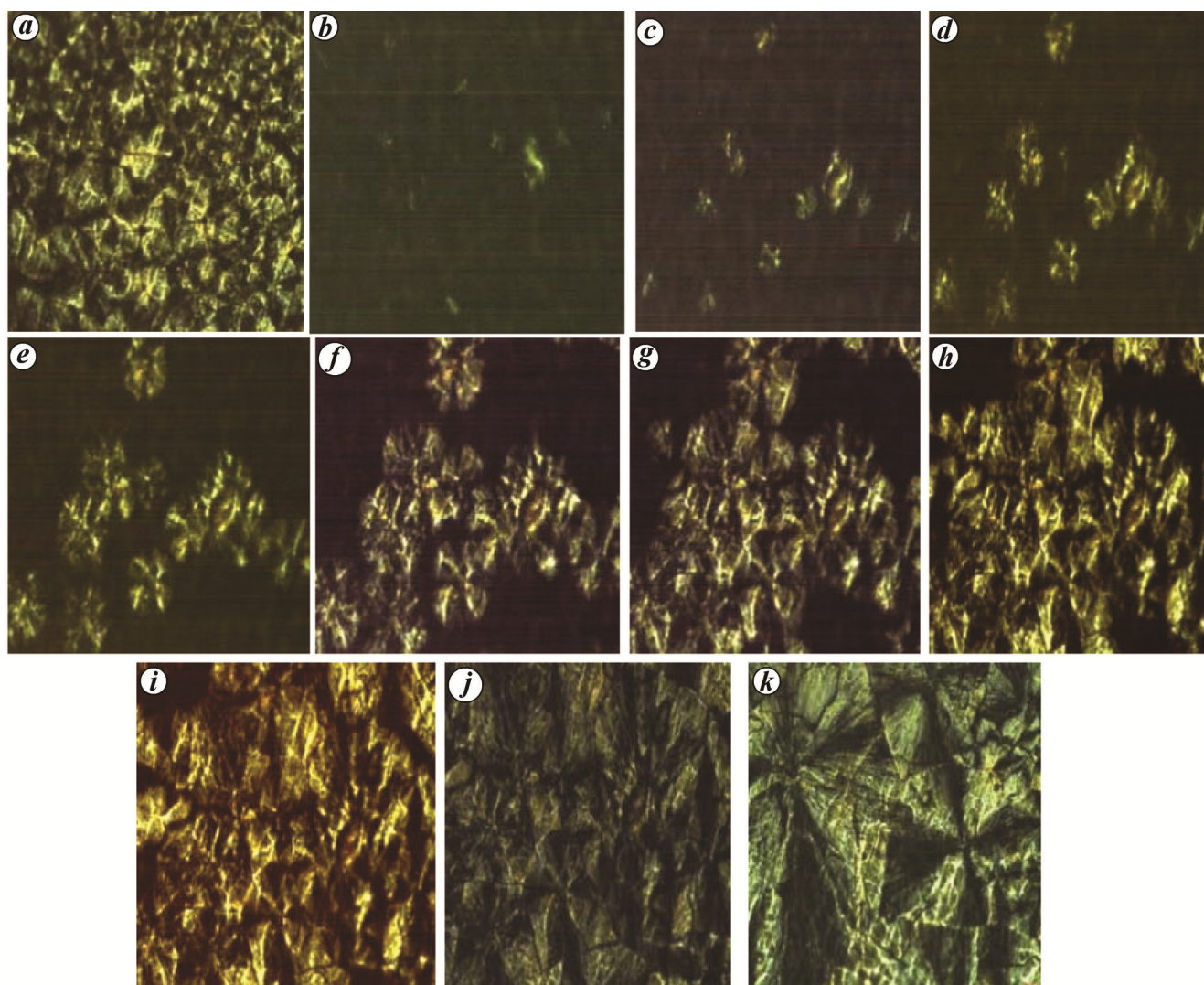


**Figure 3.** Enlarged ( $\times 1600$ ) polarized optical microscopic (POM) images exhibiting growth of spherulites in pristine PEO (*a*) before melting, 27°C, (*b*) melted, after 113 sec, at 53°C, (*c*) after 118 sec, (*d*) after 123 sec at 52°C, (*e*) after 128 sec, (*f*) after 133 sec, (*g*) after 138 sec, (*h*) after 143 sec, (*i*) after 148 sec, (*j*) after 446 sec, 32°C and (*k*) after cooling to room temperature, 27°C.

spherulites in filler-free system is about 50–100  $\mu\text{m}$ . The largest size is found in the system of  $\text{Al}_2\text{O}_3$  with grain size 10  $\mu\text{m}$ .

The addition of filler particles has a major influence on both stages of spherulite growth and act as nuclei for the growth. Some particles may act as nuclei for the spherulites, while the remainder may prevent the recrystallization tendency of PEO polymer chains through Lewis acid–base interactions with cations and anions present in the system, which results in a decrease in the growth rate of the spherulites. The increase in the number of spherulites and decrease in their size are associated with incomplete crystallization and decrease the crystalline phase in the system. This leads to an increase in the fraction of amorphous phase to crystalline phase. Also, the continuous amorphous phase in the filler-added system is much larger than in the filler-free system. This is impor-

tant for ionic transport. Thus, the filler-added system shows higher conductivities even at ambient temperatures<sup>13,22–24</sup>. Similar to the effect observed in the present study, disordering and reduction in the size of the spherulites have been observed due to the incorporation of copper-oxide filler in  $\text{P}(\text{EO})_{15}\text{LiTFSI}$  by Choi *et al.*<sup>25</sup> and organo-modified montmorillonite in fluropolymer matrix,  $\text{P}(\text{VDF}-\text{TeFE})$  by Mamun *et al.*<sup>26</sup>. Waddon and Petrovic<sup>24</sup> found retardation in the growth rate of spherulites due to incorporation of dispersed silica nanoparticles in methylethylketone with PEO.

#### FTIR characterization

Figure 6 shows the FTIR spectra of pristine PEO (curve a)  $(\text{PEO})_9\text{LiClO}_4$  electrolyte before drying (curve b), after vacuum drying in the solid state (curve c) and with the

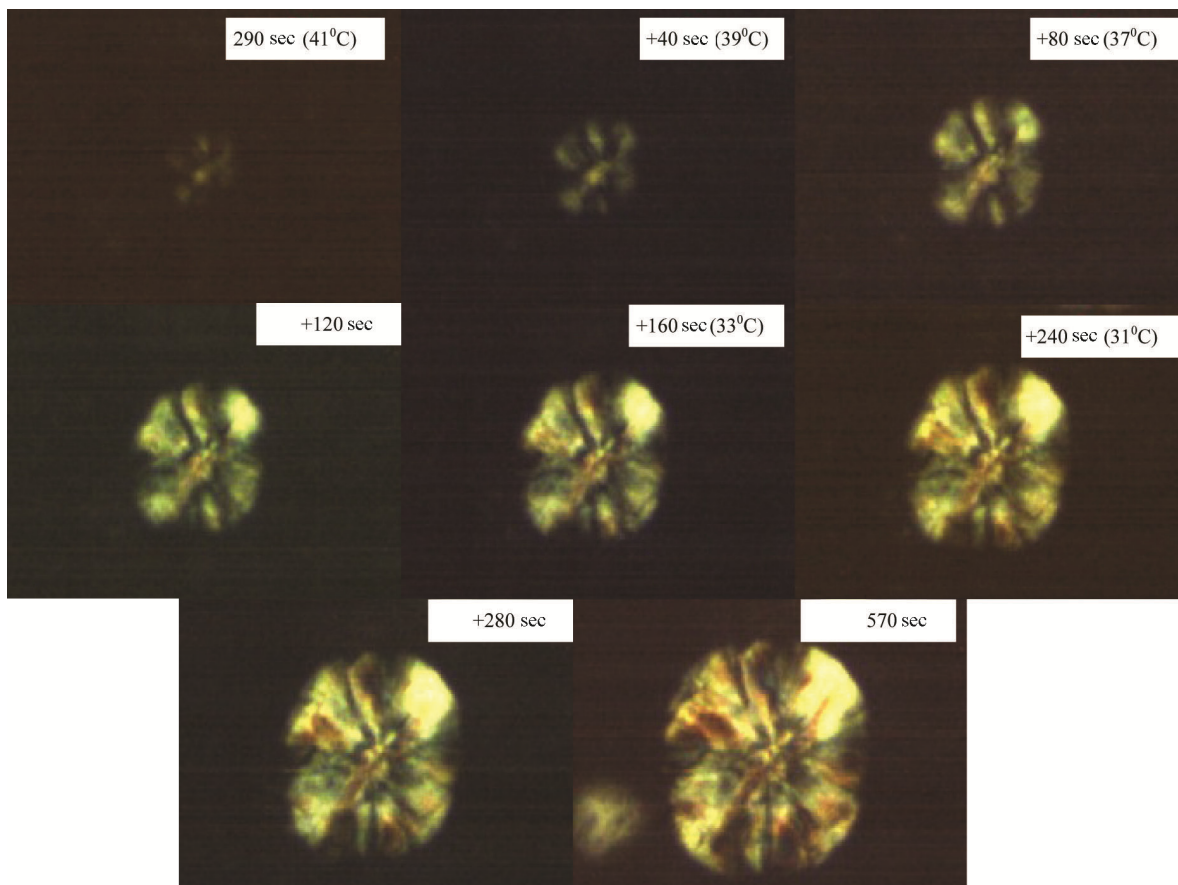


**Figure 4.** POM images showing growth of PEO spherulites in  $(\text{PEO})_9\text{LiClO}_4$  with the same magnification ( $\times 600$ ) during cooling with a rate of  $3^\circ\text{C}/\text{min}$ .

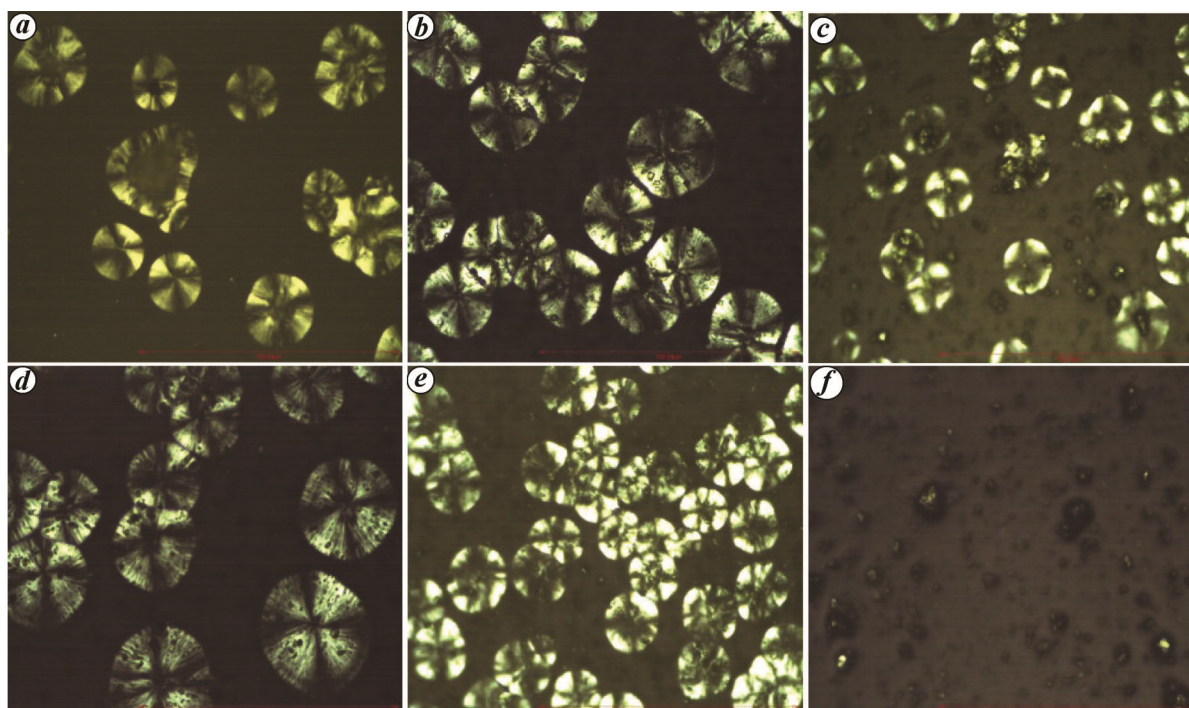


**Figure 5.** POM images of  $(\text{PEO})_9\text{LiClO}_4$  containing (a) 5 wt%, (b) 10 wt%, (c) 15 wt% of  $\text{Al}_2\text{O}_3$  particles having average grain size of  $<10\ \mu\text{m}$ , and (d) 5 wt%, (e) 10 wt%, (f) 15 wt% of  $\text{Al}_2\text{O}_3$  particles having pore size of 5.8 nm under magnification of  $\times 600$ . Scale bar is same for all images ( $100\ \mu\text{m}$ ).

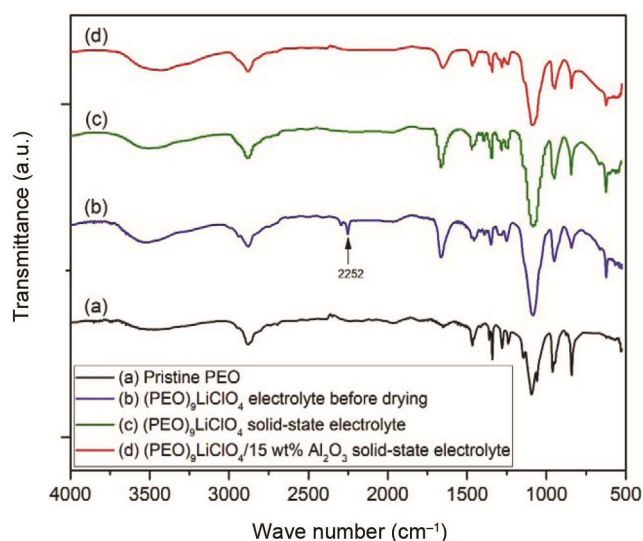


**Figure 6.** Fourier transform infrared spectra of (a) PEO, (b)  $(\text{PEO})_9\text{LiClO}_4$  before drying, (c) after drying and (d) with 15 wt% filler after drying.

15 wt% of  $\text{Al}_2\text{O}_3$  (curve d). The complete absence of traces of acetonitrile in the solid polymer electrolyte is confirmed by disappearance of the peak at  $2252\text{ cm}^{-1}$  in all the curves, except curve (b).

As can be seen from Figure 6, there is no significant difference between the positions of the peaks in the FTIR spectra of polymer electrolytes with and without the filler (curves c and d). From these results, it is clear that there is no new bond formation due to the addition of 15 wt%  $\text{Al}_2\text{O}_3$  to the  $(\text{PEO})_9\text{LiClO}_4$  electrolyte. Thus, the increase in conductivity with the addition of filler may not be associated with the formation of new bonds between the polymer matrix and the filler. According to the literature, the strong bond at  $1093\text{ cm}^{-1}$  is due to asymmetric  $-\text{C}-\text{O}-\text{C}-$  stretching and the peak that appeared at  $2884\text{ cm}^{-1}$  is due to symmetric and anti-symmetric stretching of the methylene group ( $\text{CH}_2$ ) (refs 10, 27). The band at  $1466\text{ cm}^{-1}$  is due to asymmetric  $\text{CH}_2$  bending and at  $623\text{ cm}^{-1}$  is due to rocking mode of the same group. This arises as a structural group rather than as a single unit. The broad peak at  $3500\text{ cm}^{-1}$  may be due to the stretching of  $\text{O}-\text{H}$  bonds of water molecules on the surface. This is not characteristic of the  $\text{O}-\text{H}$  groups in the structure of the electrolyte, which in turn indicates that there is no moisture present in the system.

## Conclusion

The addition of  $\text{Al}_2\text{O}_3$  on conductivity enhancement of  $(\text{PEO})_9\text{LiClO}_4$  solid polymer electrolytes was studied by observing the formation of spherulites. Nearly fourfold enhancement in ionic conductivity of the solid polymer electrolyte was achieved with the addition of 15 wt% of

$\text{Al}_2\text{O}_3$  with pore size 5.8 nm, while smaller enhancement was observed with larger filler particles ( $<10\text{ }\mu\text{m}$ ). The clear transition from crystalline to amorphous phase was observed with the addition of nano-fillers to the polymer electrolyte. Conductivity enhancement has no connection with non-bonding of the PEO matrix with the filler particles.

- Fenton, D. E., Parker, J. M. and Wrighter, P. V., Complexes of alkali metal ions with poly (ethylene oxide). *Polymer*, 1973, **14**(11), 589–590.
- Armand, M. B., The history of polymer electrolytes. *Solid State Ionics*, 1994, **69**, 3–4.
- Colombo, F. *et al.*, Polymer-in-ceramic nanocomposite solid electrolyte for lithium metal batteries encompassing PEO-grafted  $\text{TiO}_2$  nanocrystals. *J. Electrochem. Soc.*, 2020, **167**(7), 070535–070541.
- Yap, Y. L., You, A. H. and Teo, L. L., Preparation and characterization studies of PMMA–PEO-blend solid polymer electrolytes with  $\text{SiO}_2$  filler and plasticizer for lithium ion battery. *Ionics*, 2019, **25**(7), 3087–3092.
- Zhang, D. *et al.*, Recent progress in organic–inorganic composite solid electrolytes for all-solid-state lithium batteries. *Chem. Eur. J.*, 2020, **26**(8), 1720–1736.
- Pitawala, H. M. J. C., Dissanayake, M. A. K. L., Seneviratne, V. A., Mellander, B.-E. and Albinson, I., Effect of plasticizers (EC or PC) on the ionic conductivity and thermal properties of the  $(\text{PEO})_9\text{LiTf}:\text{Al}_2\text{O}_3$  nanocomposite polymer electrolyte system. *J. Solid State Electrochem.*, 2008, **12**, 783–789.
- Wimalaweera, K. K., Seneviratne, V. A. and Dissanayake, M. A. K. L., Effect of  $\text{Al}_2\text{O}_3$  ceramic filler on thermal and transport properties of poly(ethylene oxide)-lithium perchlorate solid polymer electrolyte. *Proc. Eng.*, 2017, **215**, 109–114.
- Pradeepa, P., Edwinraj, S. and Prabhu, M. R., Effects of ceramic filler in poly(vinyl chloride)/poly(ethylmethacrylate) based polymer blend electrolytes. *Chin. Chem. Lett.*, 2015, **26**, 1191–1196.
- Croce, F., Persi, L., Scrosati, B., Fiory, F. S., Plichta, E. and Hendrickson, M. A., Role of the ceramic fillers in enhancing the transport properties of composite polymer electrolytes. *Electrochim. Acta*, 2001, **46**, 2457–2461.
- Chaurasia, S. K., Singh, R. K. and Chandra, S., Dielectric relaxation and conductivity studies on  $(\text{PEO}:\text{LiClO}_4)$  polymer electrolyte with added ionic liquid [BMIM][PF6]: evidence of ion–ion interaction. *J. Polym. Sci.: Part B*, 2011, **49**, 291–300.
- Nirmala Devi, G., Chitra, S., Selvasekarapandian, S., Premalatha, M., Monisha, S. and Saranya, J., Synthesis and characterization of dextrin-based polymer electrolytes for potential applications in energy storage devices. *Ionics*, 2017, **23**, 3377–3388.
- Zhang, Q., Liu, K., Ding, F. and Liu, X. J., Recent advances in solid polymer electrolytes for lithium batteries. *Nano Res.*, 2017, **10**, 4139–4174.
- Zhang, Y., Li, J., Huo, H. and Jiang, S., Effects of lithium perchlorate on poly(ethylene oxide) spherulite morphology and spherulite growth kinetics. *J. Appl. Polym. Sci.*, 2012, **123**, 1935–1943.
- Choi, B.-K., Optical microscopy study on the crystallization in PEO–salt polymer electrolytes. *Solid State Ionics*, 2004, **168**, 123–129.
- Dissanayake, M. A. K. L., Jayathilaka, P. A. R. D., Bokalawala, R. S. P., Albinson, I. and Mellander, B.-E., Effect of concentration and grain size of alumina filler on the ionic conductivity enhancement of the  $(\text{PEO})_9\text{LiCF}_3\text{SO}_3:\text{Al}_2\text{O}_3$  composite polymer electrolyte. *J. Power Sources*, 2003, **119**, 409–414.

16. Pan, C. Y., Feng, Q., Wang, L. J., Zhang, Q. and Chao, M., Morphology and conductivity of *in-situ* PEO–LiClO<sub>4</sub>–TiO<sub>2</sub> composite polymer electrolyte. *J. Central South Univ. Technol.*, 2007, **14**, 348–352.
17. Vignarooban, K., Dissanayake, M. A. K. L., Albinson, I. and Mellander, B.-E., Effect of TiO<sub>2</sub> nano-filler and EC plasticizer on electrical and thermal properties of poly(ethylene oxide) (PEO) based solid polymer electrolytes. *Solid State Ionics*, 2014, **266**(15), 25–28.
18. Dissanayake, M. A. K. L., Rupasinghe, W. N. S., Seneviratne, V. A., Thotawatthage, C. A. and Senadeera, G. K. R., Optimization of iodide ion conductivity and nano filler effect for efficiency enhancement in polyethylene oxide (PEO) based dye sensitized solar cells. *Electrochim. Acta*, 2014, **145**, 319–326.
19. Zhang, S., Lee, J. Y. and Hong, L., Li<sup>+</sup> conducting ‘fuzzy’ poly(ethylene oxide)–SiO<sub>2</sub> polymer composite electrolytes. *J. Power Sources*, 2004, **134**, 95–102.
20. Das, S. and Ghosh, A., Ionic conductivity and dielectric permittivity of PEO–LiClO<sub>4</sub> solid polymer electrolyte plasticized with propylene carbonate. *AIP Adv.*, 2015, **5**, 027125–027134.
21. Aziza, S. B., Woo, T. J., Kadir, M. F. Z. and Ahmed, H. M., A conceptual review on polymer electrolytes and ion transport models. *J. Sci.: Adv. Mater. Devices*, 2018, **3**(1), 1–17.
22. Gránásy, L., Puzstai, T., Tegze, G., Warren, J. A. and Douglas, J. F., Growth and form of spherulites. *Phys. Rev.*, 2005, **E72**, 011605–011615.
23. Raimo, M., Estimation of polymer nucleation and growth rates, by overall DSC crystallization rates. *Polym. J.*, 2011, **43**, 78–83.
24. Waddon, A. J. and Petrovic, Z. S., Spherulite crystallization in poly(ethylene oxide)–silica nanocomposites. Retardation of growth rates through reduced molecular mobility, *Polymer J.*, 2002, **34**(12), 876–881.
25. Choi, B. N., Yang, J. H., Kim, Y. S. and Chung, C. H., Effect of morphological change of copper-oxide fillers on the performance of solid polymer electrolytes for lithium–metal polymer batteries. *RSC Adv.*, 2019, **9**, 21760–21770.
26. Mamun, M. A. A., Kasahara, Y., Tasaki, T. and Fujimori, A., Spherulitic formation and characterization of partially fluorinated copolymers and their nanohybrids with functional fillers. *Polym. Eng. Sci.*, 2017, **57**, 161–171.
27. Pucić, I. and Jurkin, T., FTIR assessment of poly(ethyleneoxide) irradiated in solid state, melt and aqueous solution. *Radiat. Phys. Chem.*, 2012, **81**, 1426–1429.

Received 27 October 2020; revised accepted 17 November 2020

doi: 10.18520/cs/v120/i5/900-906